

Short-range correlation physics at low RG resolution

Anthony Tropiano¹, Scott Bogner², Dick Furnstahl¹

¹Ohio State University, ²Michigan State University

NUCLEI Annual Meeting

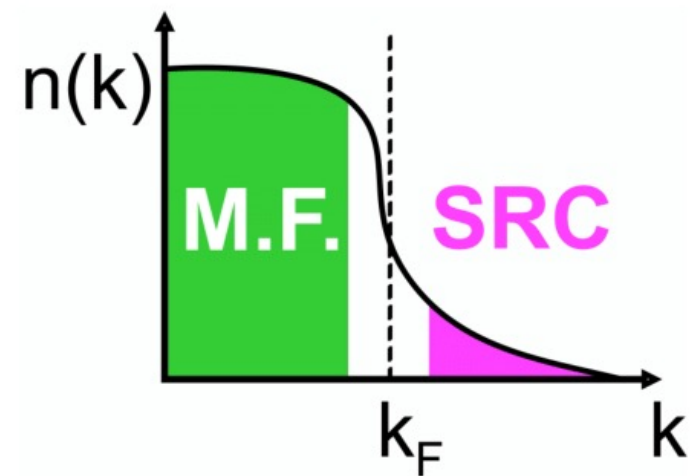
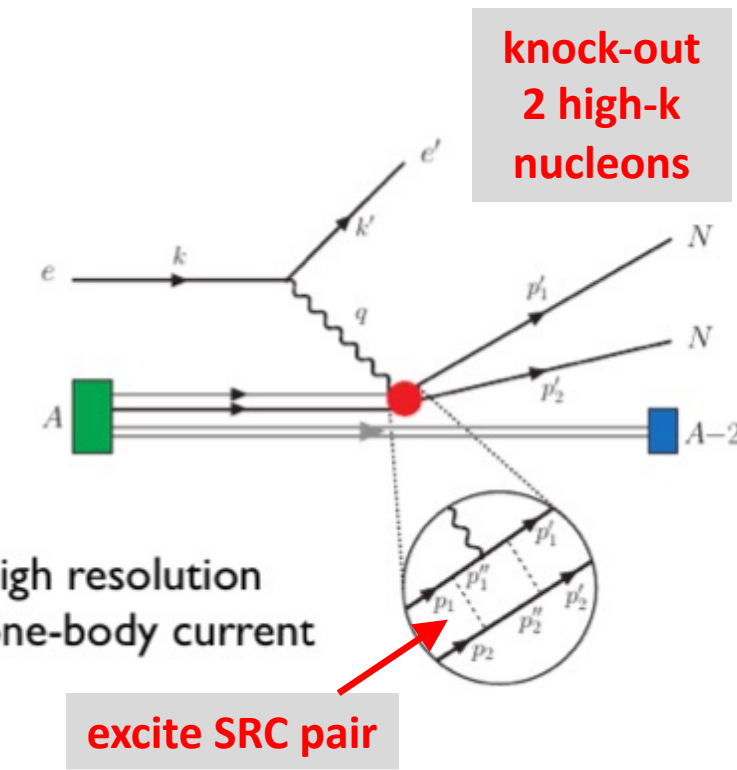
June 2, 2021

ajt, S.K. Bogner, and R.J. Furnstahl, arXiv:2105.13936



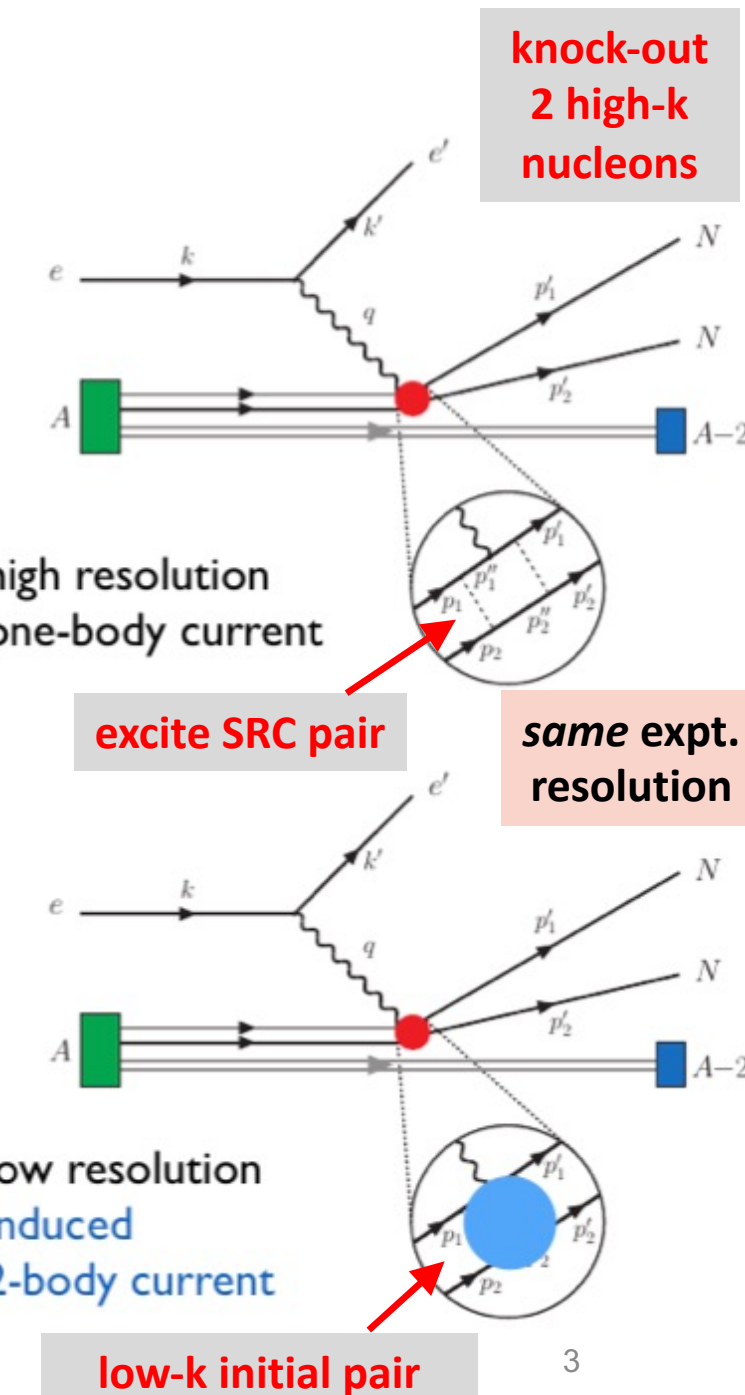
Motivation

- Recent experiments have been able to isolate processes where short-range correlation (SRC) physics is dominant and well accounted for by SRC phenomenology
- SRC physics at **high RG resolution**
 - SRC pairs are components in the nuclear wave function with relative momenta above the Fermi momentum



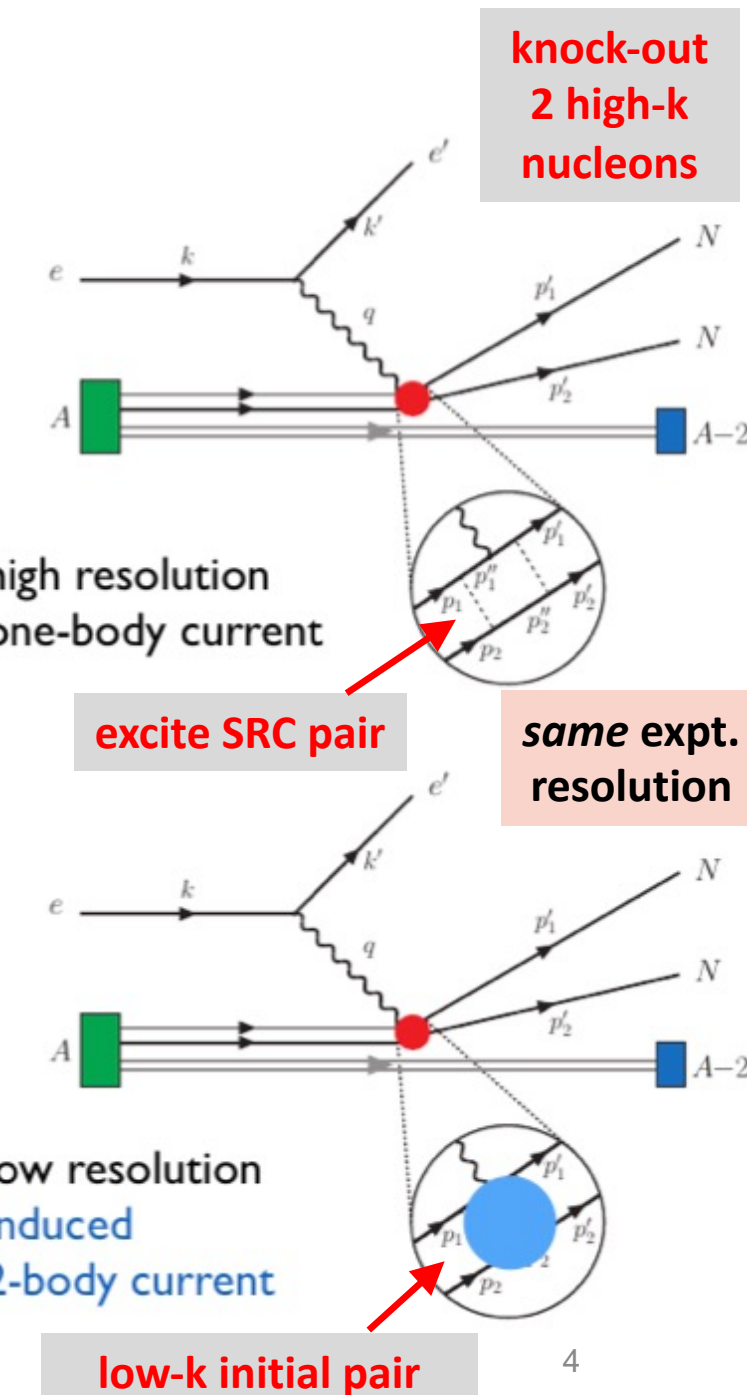
Motivation

- Recent experiments have been able to isolate processes where short-range correlation (SRC) physics is dominant and well accounted for by SRC phenomenology
- SRC physics at **low RG resolution**
 - The SRC *physics* is shifted into the reaction operators from the nuclear wave function (which becomes soft)
 - Operators do not become hard which simplifies calculations



Motivation

- Recent experiments have been able to isolate processes where short-range correlation (SRC) physics is dominant and well accounted for by SRC phenomenology
- SRC physics at **low RG resolution**
 - The SRC *physics* is shifted into the reaction operators from the nuclear wave function (which becomes soft)
 - Operators do not become hard which simplifies calculations
- Experimental resolution (set by momentum of probe) is the same in both pictures
- Same observables but different physical interpretation!



Similarity Renormalization Group (SRG)

- AV18 wave function has significant SRC
- What happens to the wave function at low RG resolution?
- Use SRG to unitarily evolve to low RG resolution where λ gives the decoupling scale

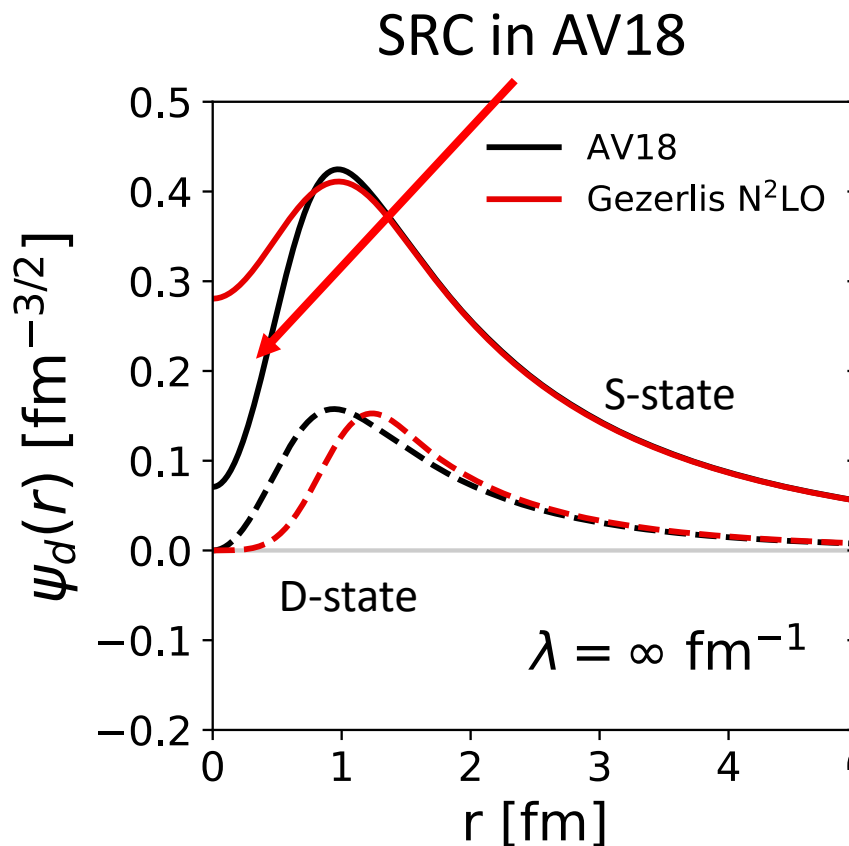


Fig. 1: SRG evolution of deuteron wave function in coordinate space for AV18 and Gezerlis N2LO¹.

Similarity Renormalization Group (SRG)

- SRC physics in AV18 is gone from wave function at low RG resolution
- Deuteron wave functions become soft and D-state probability goes down
- Observables such as asymptotic D-S ratio are the same

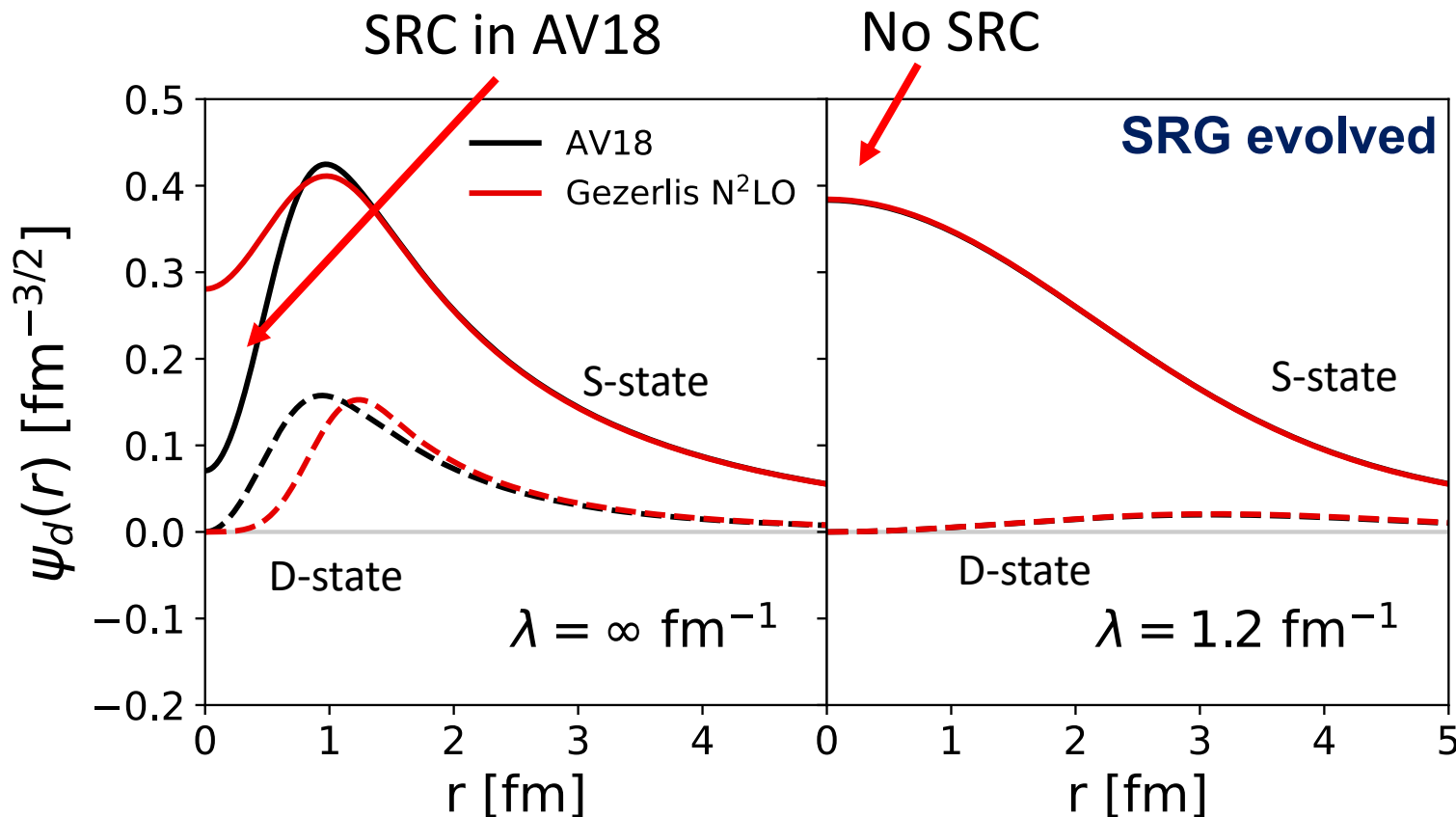


Fig. 1: SRG evolution of deuteron wave function in coordinate space for AV18 and Gezerlis N2LO¹.

Momentum distributions at low RG resolution

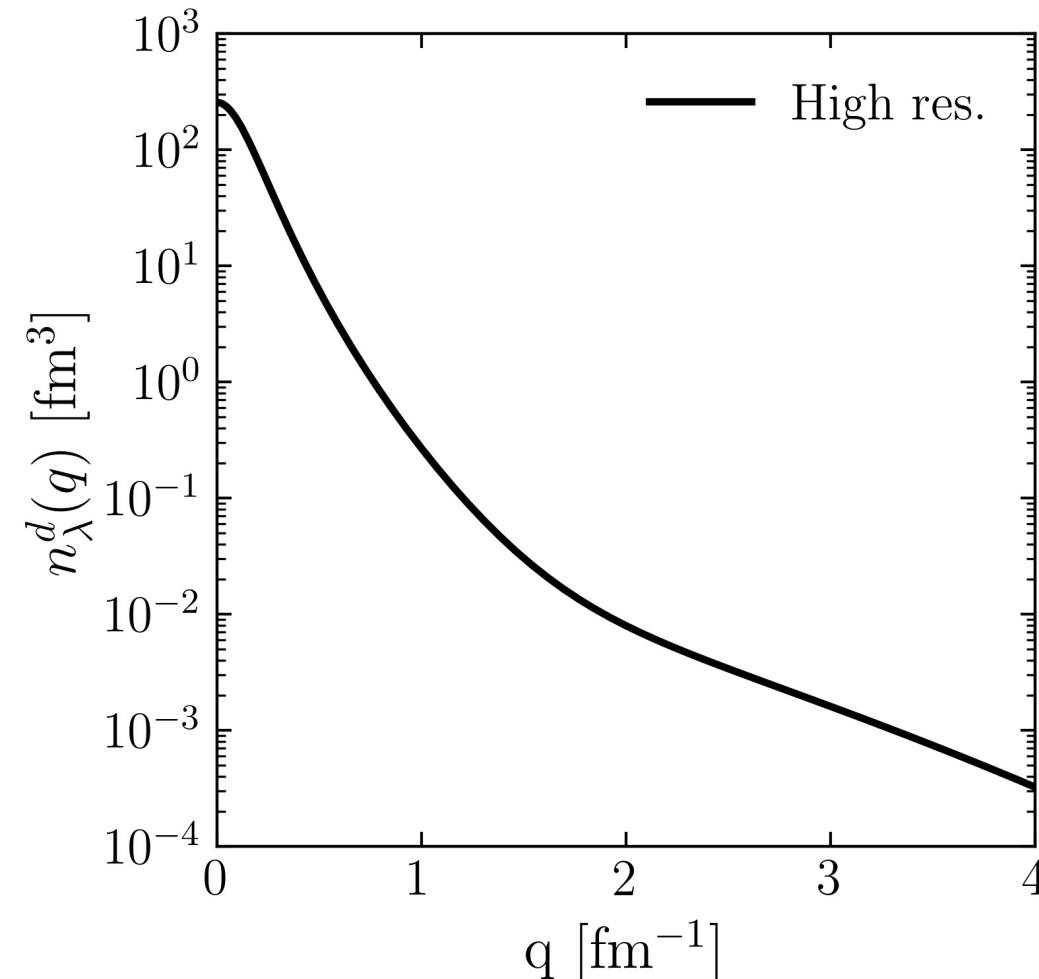
- Soft wave functions at low RG resolution
 - Where does the SRC physics go?

Momentum distributions at low RG resolution

- Soft wave functions at low RG resolution
 - Where does the SRC physics go?
- SRC physics shifts to the operators $\langle \psi_f^{hi} | U_\lambda^\dagger U_\lambda O^{hi} U_\lambda^\dagger U_\lambda | \psi_i^{hi} \rangle$
- Apply SRG transformations to momentum distribution operator

$$n^{hi}(\mathbf{q}) = a_{\mathbf{q}}^\dagger a_{\mathbf{q}}$$
$$U_\lambda = 1 + \frac{1}{4} \sum_{K, \mathbf{k}, \mathbf{k}'} \delta U_\lambda^{(2)}(\mathbf{k}, \mathbf{k}') a_{\frac{K}{2}+\mathbf{k}}^\dagger a_{\frac{K}{2}-\mathbf{k}}^\dagger a_{\frac{K}{2}-\mathbf{k}'} a_{\frac{K}{2}+\mathbf{k}'} + \dots$$

Momentum distributions at low RG resolution



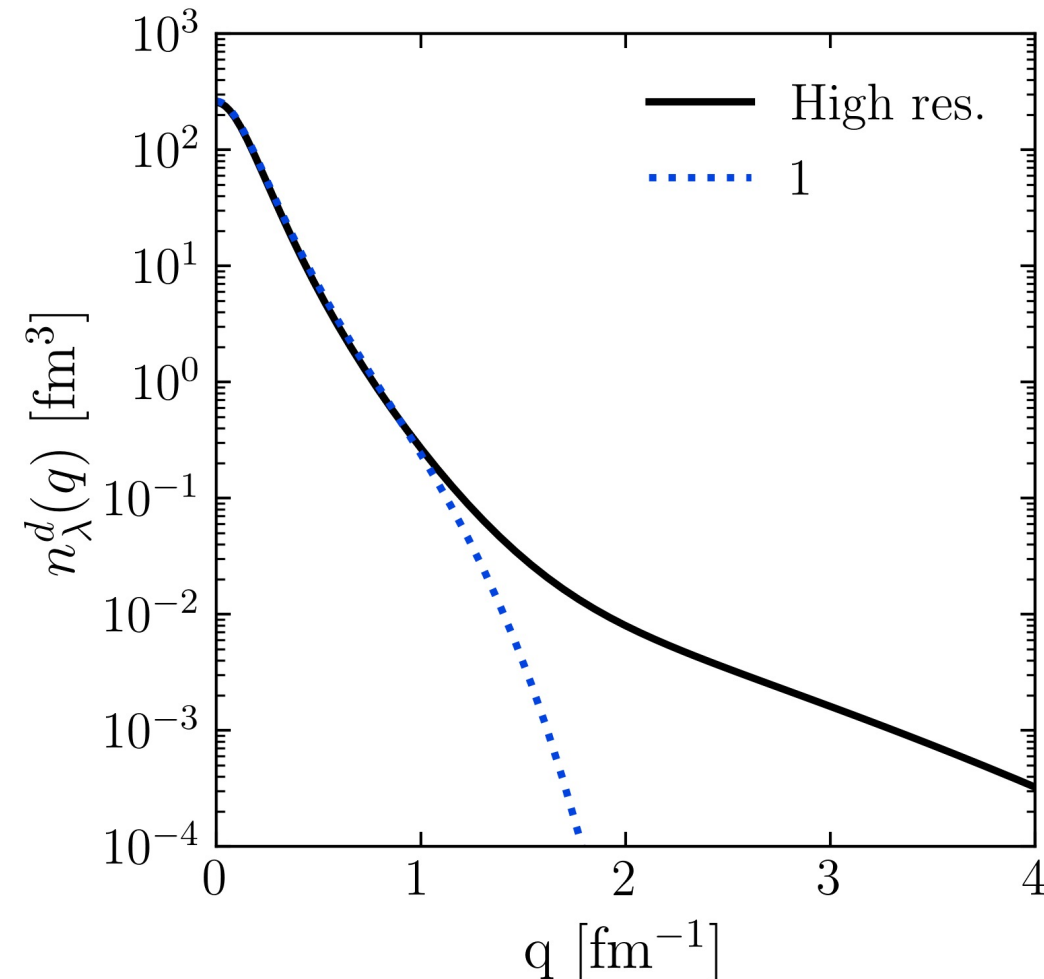
- Deuteron example

$$n^{lo}(\mathbf{q}) = (1 + \delta U) a_{\mathbf{q}}^\dagger a_{\mathbf{q}} (1 + \delta U^\dagger)$$

$$\langle \psi_d^{hi} | a_{\mathbf{q}}^\dagger a_{\mathbf{q}} | \psi_d^{hi} \rangle$$

Fig. 2: Contributions to deuteron momentum distribution with AV18 and $\lambda = 1.35$ fm⁻¹.

Momentum distributions at low RG resolution



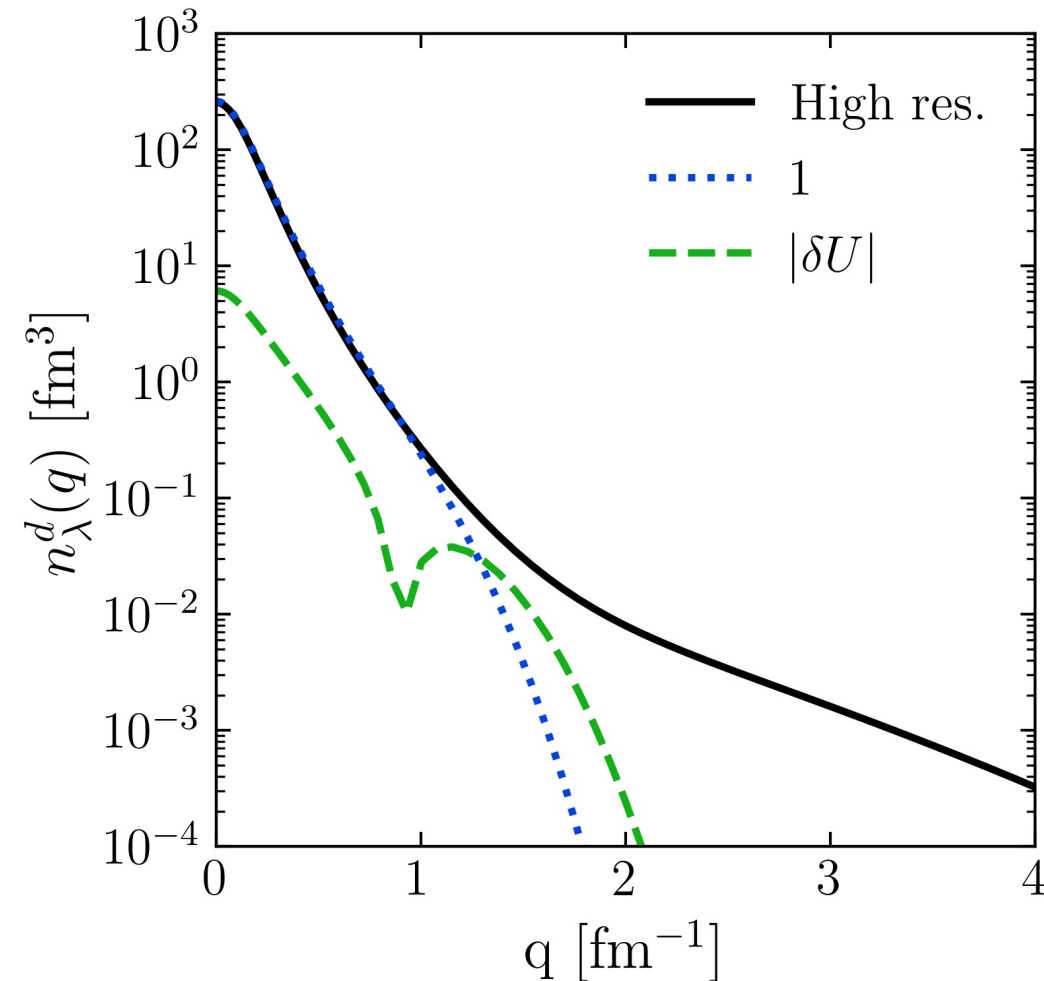
- Deuteron example

$$n^{lo}(\mathbf{q}) = (1 + \delta U) a_{\mathbf{q}}^\dagger a_{\mathbf{q}} (1 + \delta U^\dagger)$$

$$\begin{aligned}\langle \psi_d^{hi} | a_{\mathbf{q}}^\dagger a_{\mathbf{q}} | \psi_d^{hi} \rangle \\ \langle \psi_d^{lo} | a_{\mathbf{q}}^\dagger a_{\mathbf{q}} | \psi_d^{lo} \rangle\end{aligned}$$

Fig. 2: Contributions to deuteron momentum distribution with AV18 and $\lambda = 1.35$ fm⁻¹.

Momentum distributions at low RG resolution



- Deuteron example

$$n^{lo}(\mathbf{q}) = (1 + \delta U) a_{\mathbf{q}}^\dagger a_{\mathbf{q}} (1 + \delta U^\dagger)$$

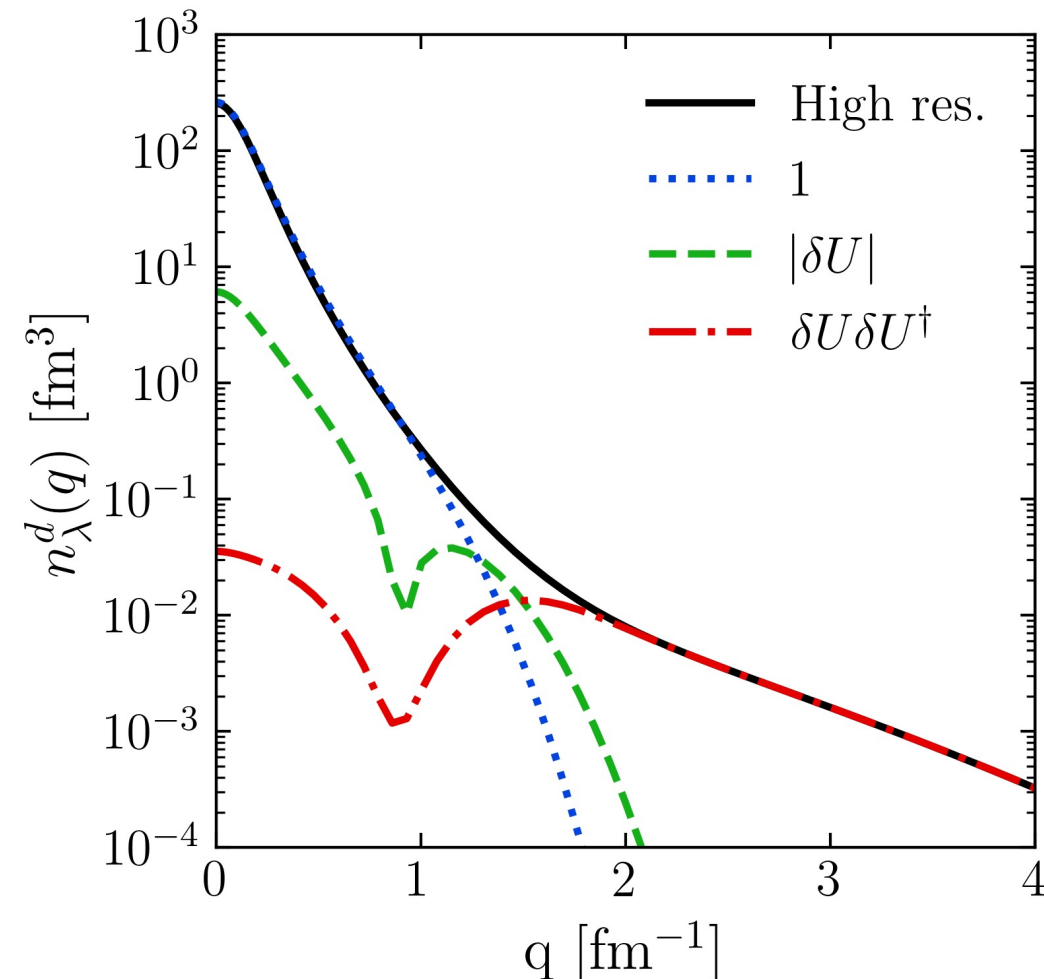
$$\langle \psi_d^{hi} | a_{\mathbf{q}}^\dagger a_{\mathbf{q}} | \psi_d^{hi} \rangle$$

$$\langle \psi_d^{lo} | a_{\mathbf{q}}^\dagger a_{\mathbf{q}} | \psi_d^{lo} \rangle$$

$$\langle \psi_d^{lo} | \delta U a_{\mathbf{q}}^\dagger a_{\mathbf{q}} + a_{\mathbf{q}}^\dagger a_{\mathbf{q}} \delta U^\dagger | \psi_d^{lo} \rangle$$

Fig. 2: Contributions to deuteron momentum distribution with AV18 and $\lambda = 1.35$ fm⁻¹.

Momentum distributions at low RG resolution



- Deuteron example

$$n^{lo}(\mathbf{q}) = (1 + \delta U) a_{\mathbf{q}}^\dagger a_{\mathbf{q}} (1 + \delta U^\dagger)$$

$$\langle \psi_d^{hi} | a_{\mathbf{q}}^\dagger a_{\mathbf{q}} | \psi_d^{hi} \rangle$$

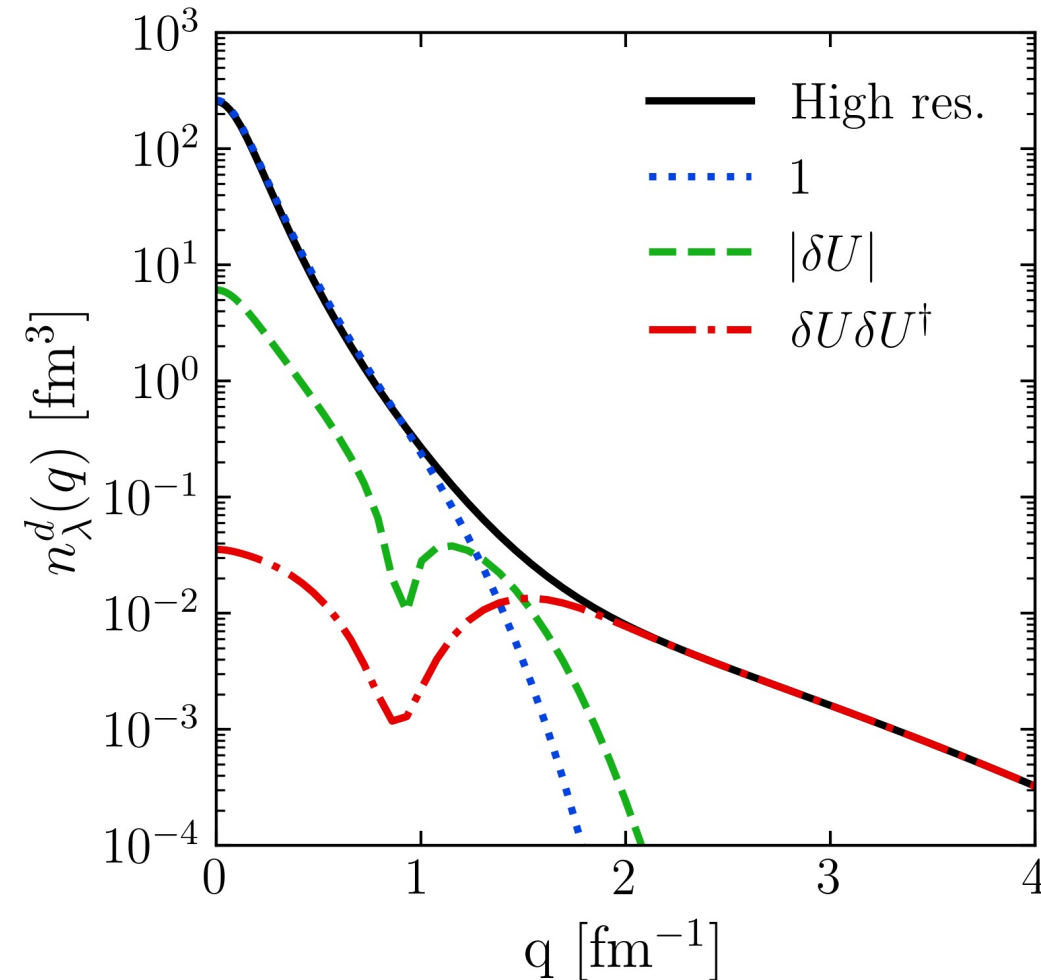
$$\langle \psi_d^{lo} | a_{\mathbf{q}}^\dagger a_{\mathbf{q}} | \psi_d^{lo} \rangle$$

$$\langle \psi_d^{lo} | \delta U a_{\mathbf{q}}^\dagger a_{\mathbf{q}} + a_{\mathbf{q}}^\dagger a_{\mathbf{q}} \delta U^\dagger | \psi_d^{lo} \rangle$$

$$\langle \psi_d^{lo} | \delta U a_{\mathbf{q}}^\dagger a_{\mathbf{q}} \delta U^\dagger | \psi_d^{lo} \rangle$$

Fig. 2: Contributions to deuteron momentum distribution with AV18 and $\lambda = 1.35$ fm⁻¹.

Momentum distributions at low RG resolution

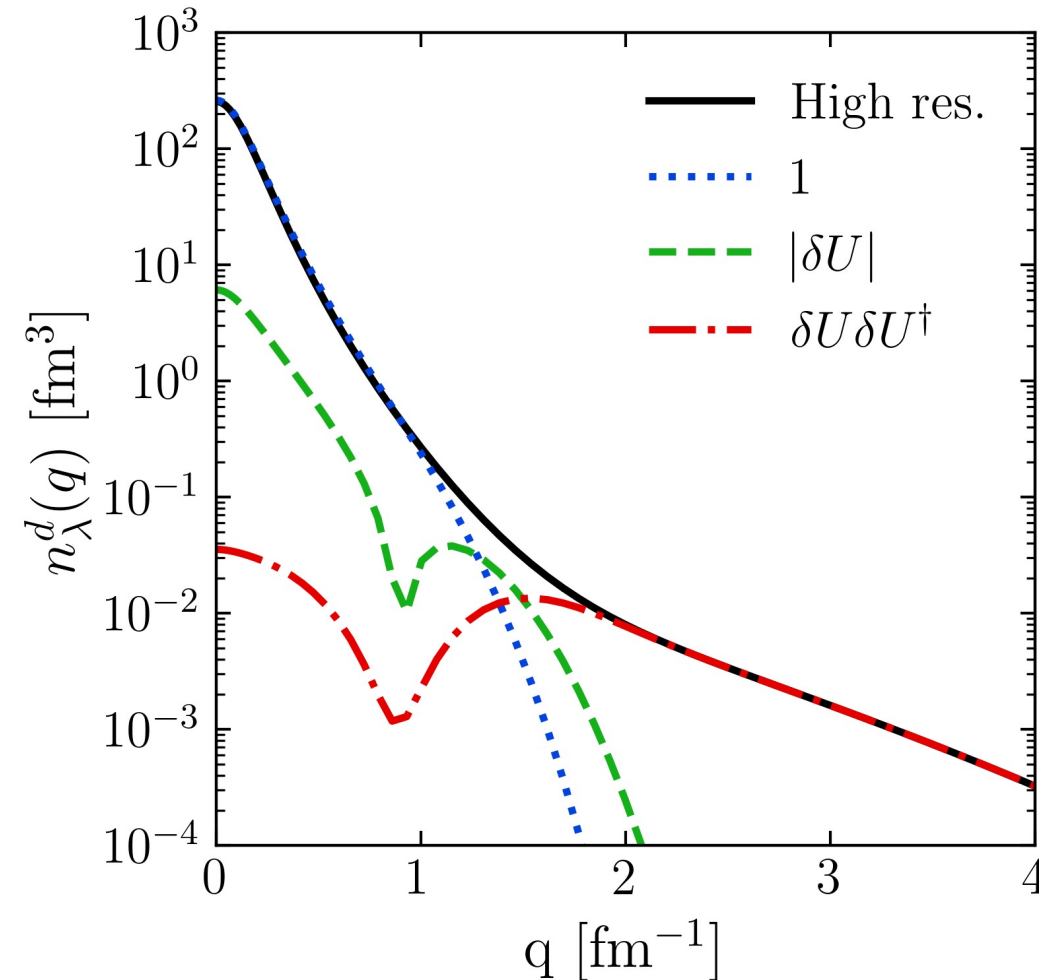


- For high- q , the $\delta U_\lambda \delta U_\lambda^\dagger$ 2-body term dominates

$$\approx \sum_{K,k,k'} \delta U_\lambda(\mathbf{k}, \mathbf{q}) \delta U_\lambda^\dagger(\mathbf{q}, \mathbf{k}') a_{\frac{\mathbf{K}}{2}+\mathbf{k}}^\dagger a_{\frac{\mathbf{K}}{2}-\mathbf{k}}^\dagger a_{\frac{\mathbf{K}}{2}-\mathbf{k}'} a_{\frac{\mathbf{K}}{2}+\mathbf{k}'}$$

Fig. 2: Contributions to deuteron momentum distribution with AV18 and $\lambda = 1.35$ fm⁻¹.

Momentum distributions at low RG resolution



- For high- q , the $\delta U_\lambda \delta U_\lambda^\dagger$ 2-body term dominates

$$\approx \sum_{\mathbf{K}, \mathbf{k}, \mathbf{k}'} \delta U_\lambda(\mathbf{k}, \mathbf{q}) \delta U_\lambda^\dagger(\mathbf{q}, \mathbf{k}') a_{\frac{\mathbf{K}}{2} + \mathbf{k}}^\dagger a_{\frac{\mathbf{K}}{2} - \mathbf{k}}^\dagger a_{\frac{\mathbf{K}}{2} - \mathbf{k}'} a_{\frac{\mathbf{K}}{2} + \mathbf{k}'}$$



Factorization: $\delta U_\lambda(\mathbf{k}, \mathbf{q}) \approx F_\lambda^{lo}(\mathbf{k}) F_\lambda^{hi}(\mathbf{q})$

$$\approx |F_\lambda^{hi}(\mathbf{q})|^2 \sum_{\mathbf{K}, \mathbf{k}, \mathbf{k}'}^{\lambda} F_\lambda^{lo}(\mathbf{k}) F_\lambda^{lo}(\mathbf{k}') a_{\frac{\mathbf{K}}{2} + \mathbf{k}}^\dagger a_{\frac{\mathbf{K}}{2} - \mathbf{k}}^\dagger a_{\frac{\mathbf{K}}{2} - \mathbf{k}'} a_{\frac{\mathbf{K}}{2} + \mathbf{k}'}$$



Fig. 2: Contributions to deuteron momentum distribution with AV18 and $\lambda = 1.35$ fm⁻¹.

Momentum distributions at low RG resolution

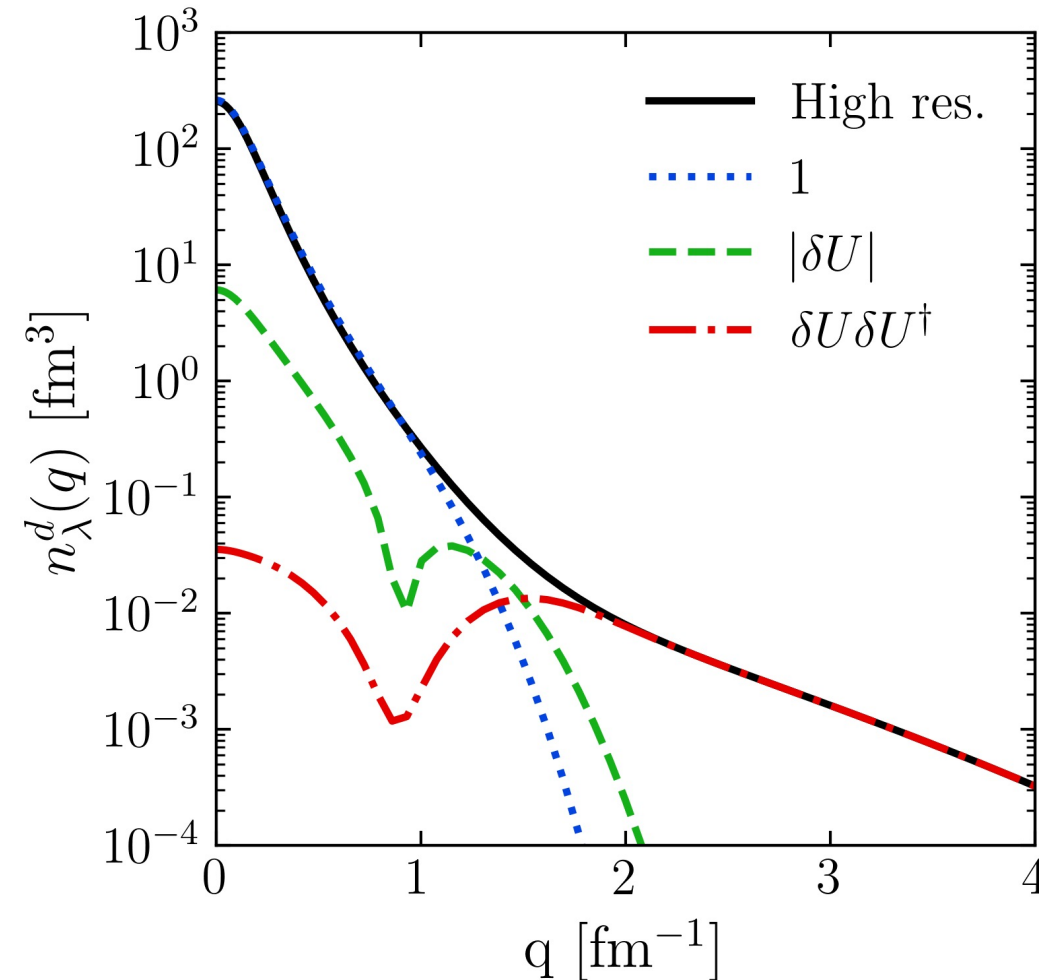


Fig. 2: Contributions to deuteron momentum distribution with AV18 and $\lambda = 1.35$ fm⁻¹.

- For high- q , the $\delta U_\lambda \delta U_\lambda^\dagger$ 2-body term dominates

$$\approx \sum \delta U_\lambda(k, q) \delta U_\lambda^\dagger(q, k') a_{\frac{K}{2}+k}^\dagger a_{\frac{K}{2}-k}^\dagger a_{\frac{K}{2}-k'} a_{\frac{K}{2}+k'}$$

Apply this strategy to nuclear momentum distributions using local density approximation (LDA)!

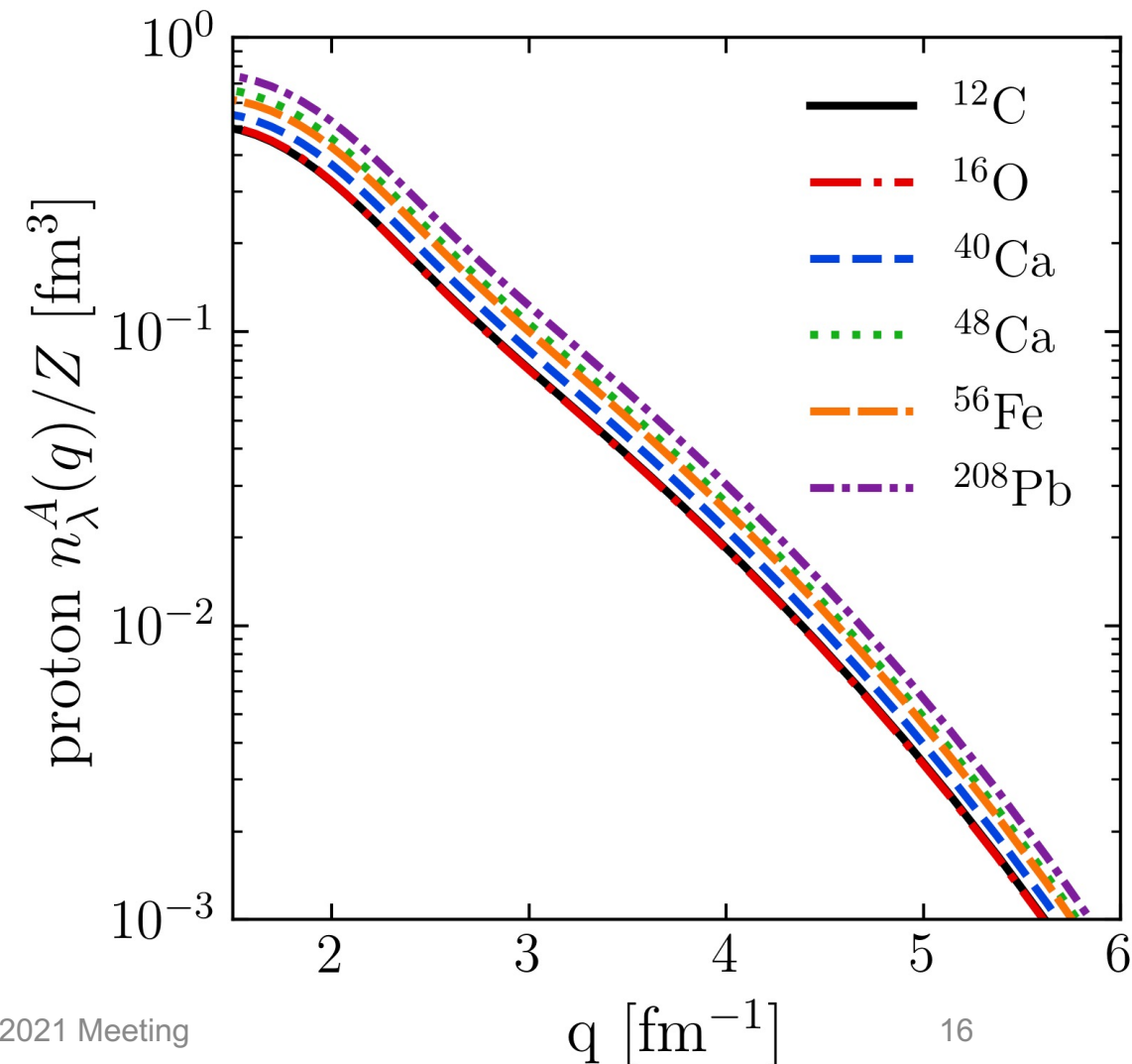
$$\approx |F_\lambda^{lo}(q)|^2 \sum_{K,k,k'} F_\lambda^{lo}(k) F_\lambda^{lo}(k') a_{\frac{K}{2}+k}^\dagger a_{\frac{K}{2}-k}^\dagger a_{\frac{K}{2}-k'} a_{\frac{K}{2}+k'}$$

$$F_\lambda^{hi}(q)$$

LDA results

- **Universality**
 - High- q tail collapses to universal function $\approx |F_\lambda^{hi}(\mathbf{q})|^2$ fixed by 2-body
 - Results are insensitive to type of density

Fig. 3: Proton momentum distribution under LDA with AV18, $\lambda = 1.35 \text{ fm}^{-1}$, and densities from Skyrme EDF SLy4 using the HFBRAD code¹.



LDA results

- Low RG resolution calculations reproduce momentum distributions of AV18 data¹ (high RG resolution calculation)
- Low RG works well with simple approximations and is systematically improvable

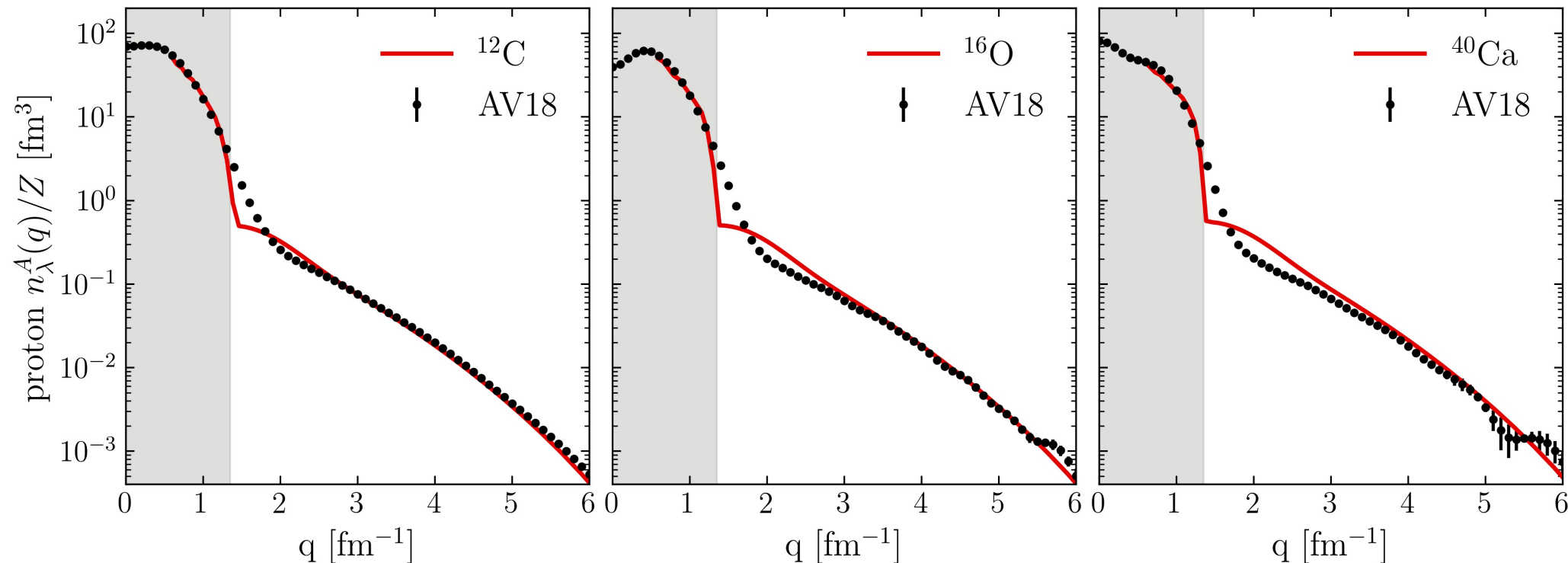


Fig. 4: Proton momentum distributions for ¹²C, ¹⁶O, and ⁴⁰Ca under LDA with AV18 and $\lambda = 1.35$ fm⁻¹.

LDA results

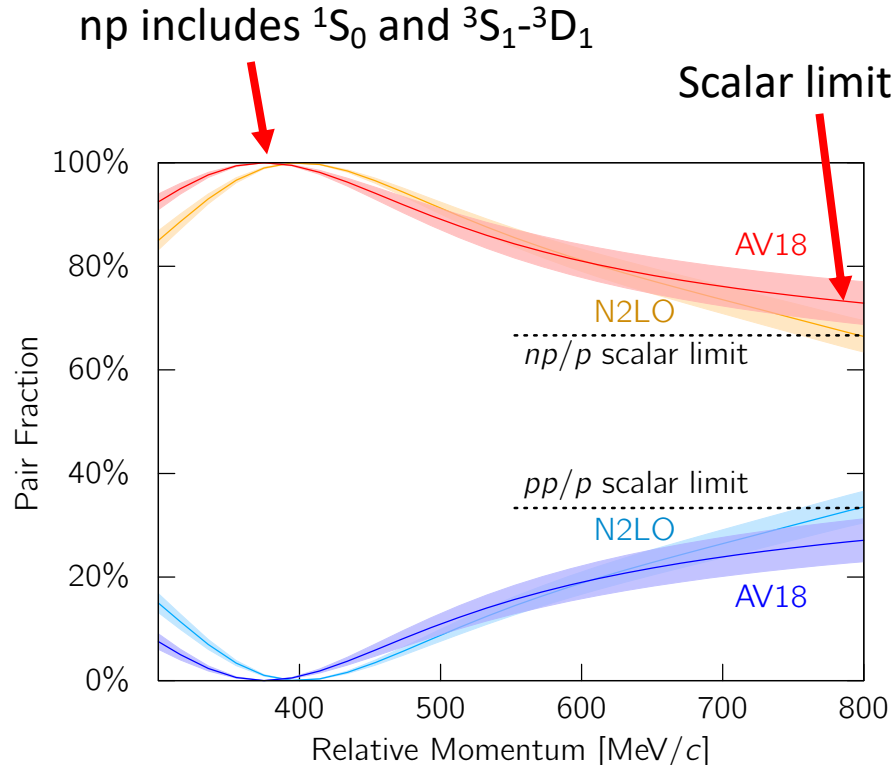
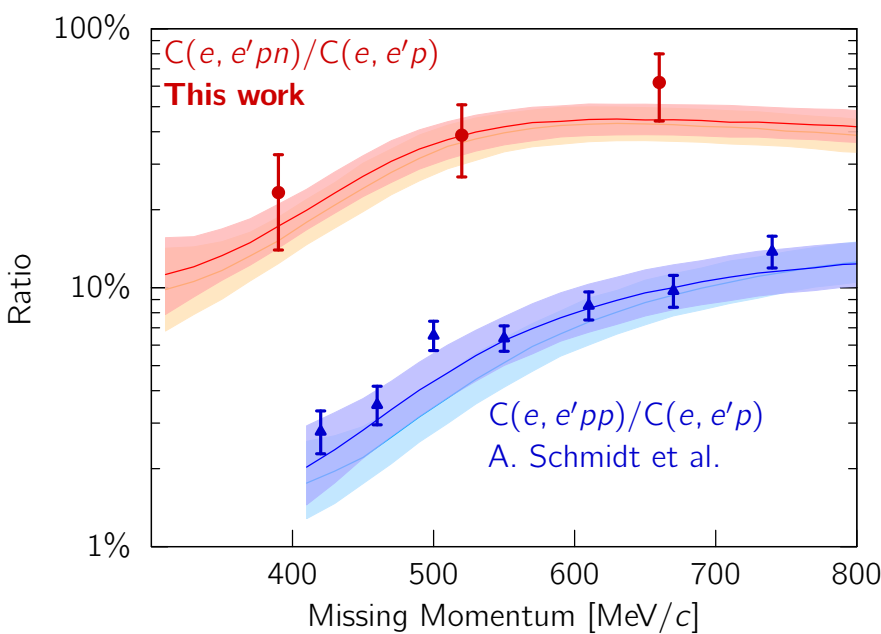


Fig. 5: (a) Ratio of two-nucleon to single-nucleon electron-scattering cross sections for carbon as a function of missing momentum. (b) Fraction of np to p and pp to p pairs versus the relative momentum. Figure from CLAS collaboration publication¹.

- At **high RG resolution**, the tensor force and the repulsive core of the NN interaction kicks nucleon pairs into SRCs
- np dominates because the tensor force requires spin triplet pairs (pp are spin singlets)
- **Do we describe this physics at low RG resolution?**

¹I. Korover et al. (CLAS), arXiv:2004.07304 (2014)

LDA results

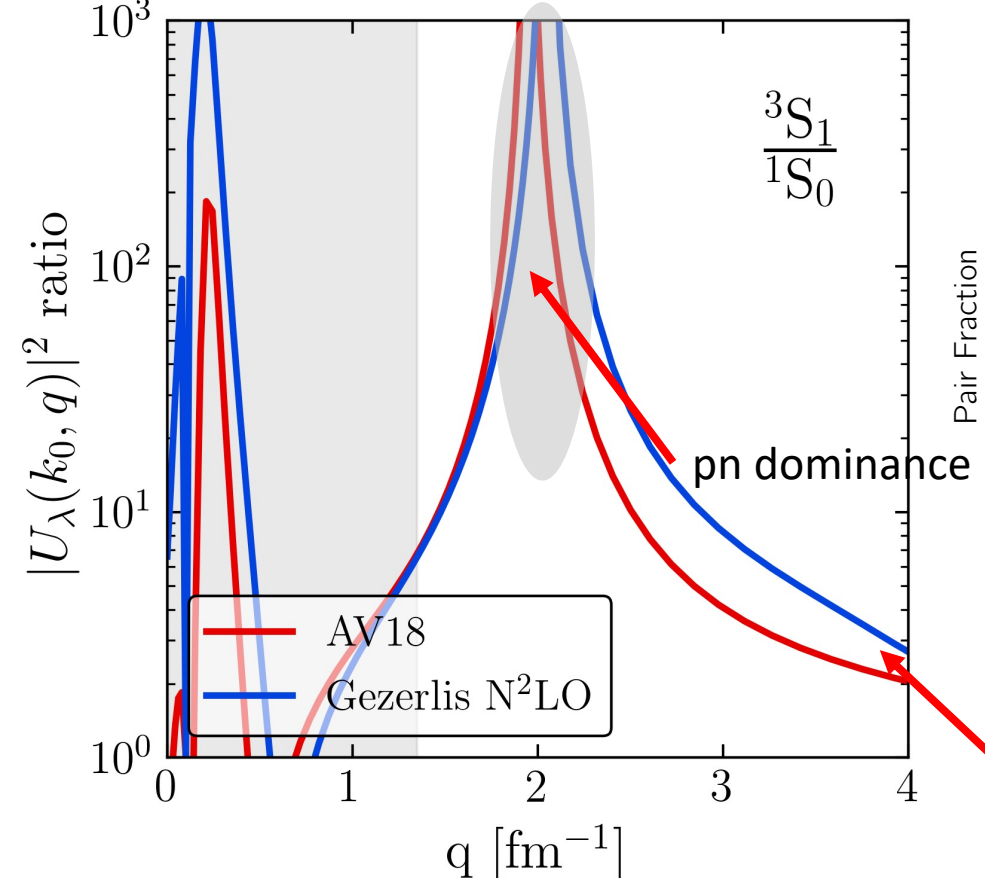
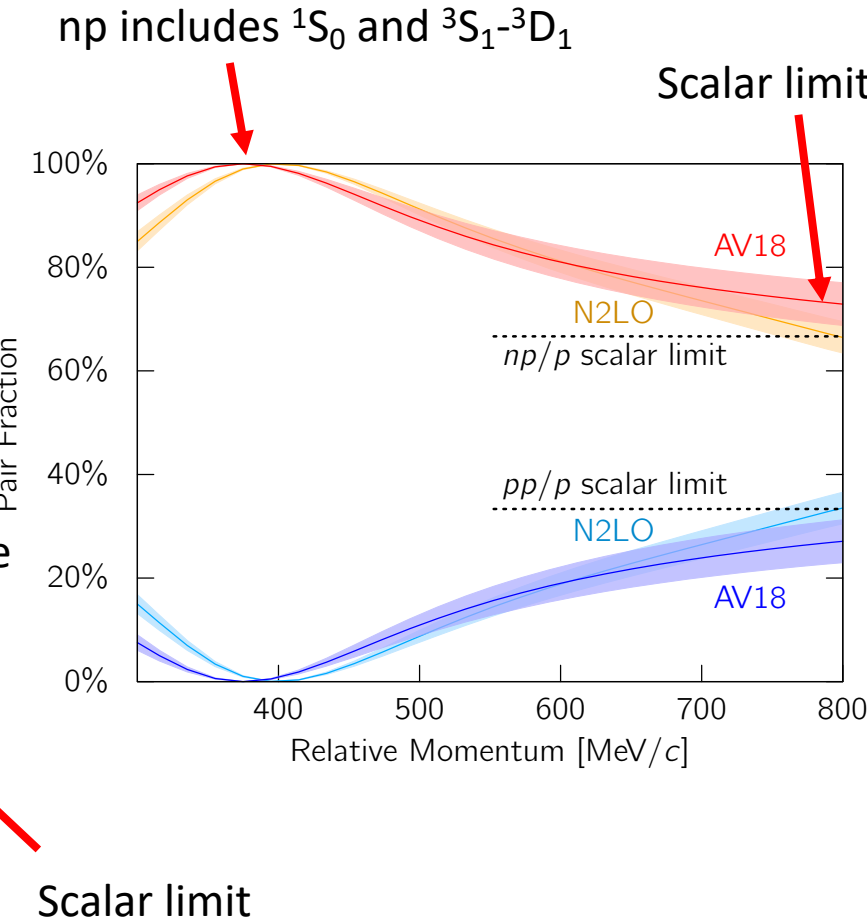
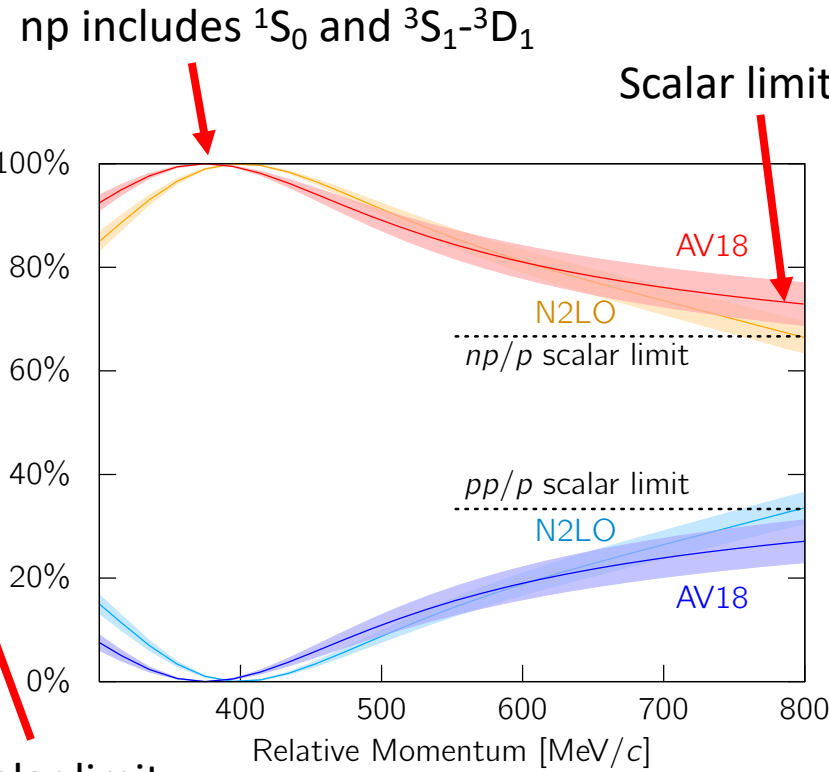
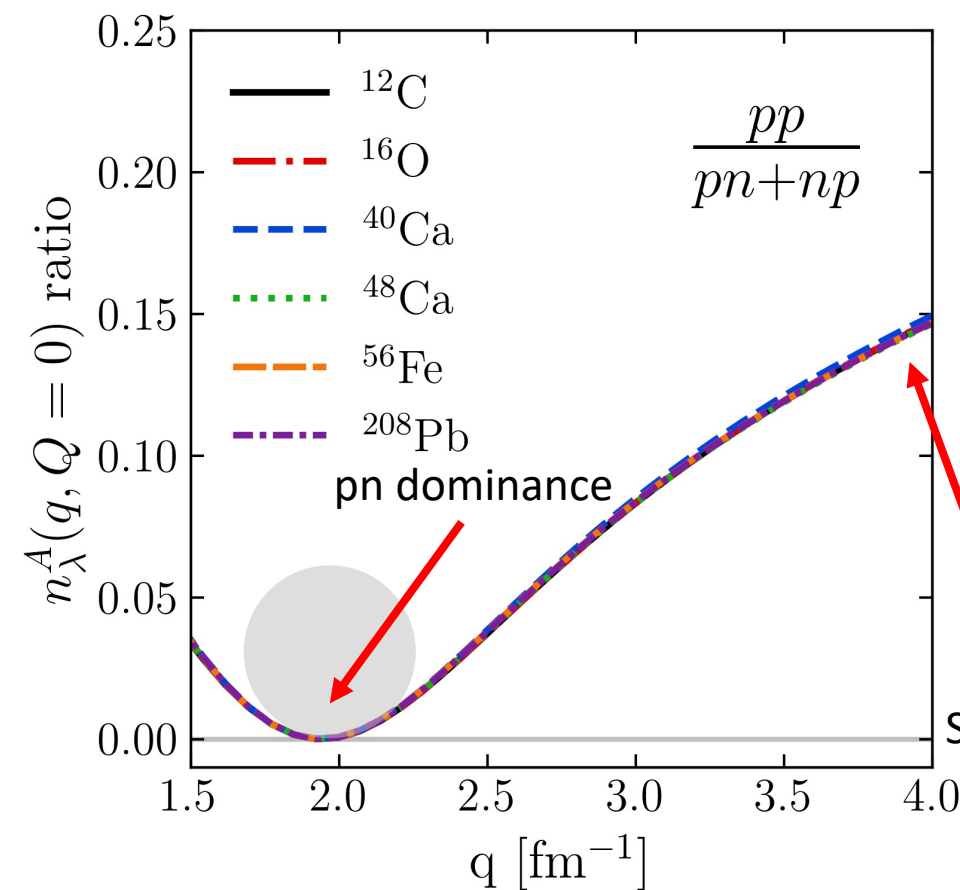


Fig. 6: $^3\text{S}_1$ to $^1\text{S}_0$ ratio of SRG-evolved momentum projection operators $a_q^\dagger a_q$.



- At **low RG resolution**, SRCs are suppressed in the wave function
- Consider the ratio of $^3\text{S}_1$ - $^3\text{D}_1$ to $^1\text{S}_0$ evolved momentum projection operator $a_q^\dagger a_q$
- This physics is established in the 2-body system!
- Can apply to any nucleus!

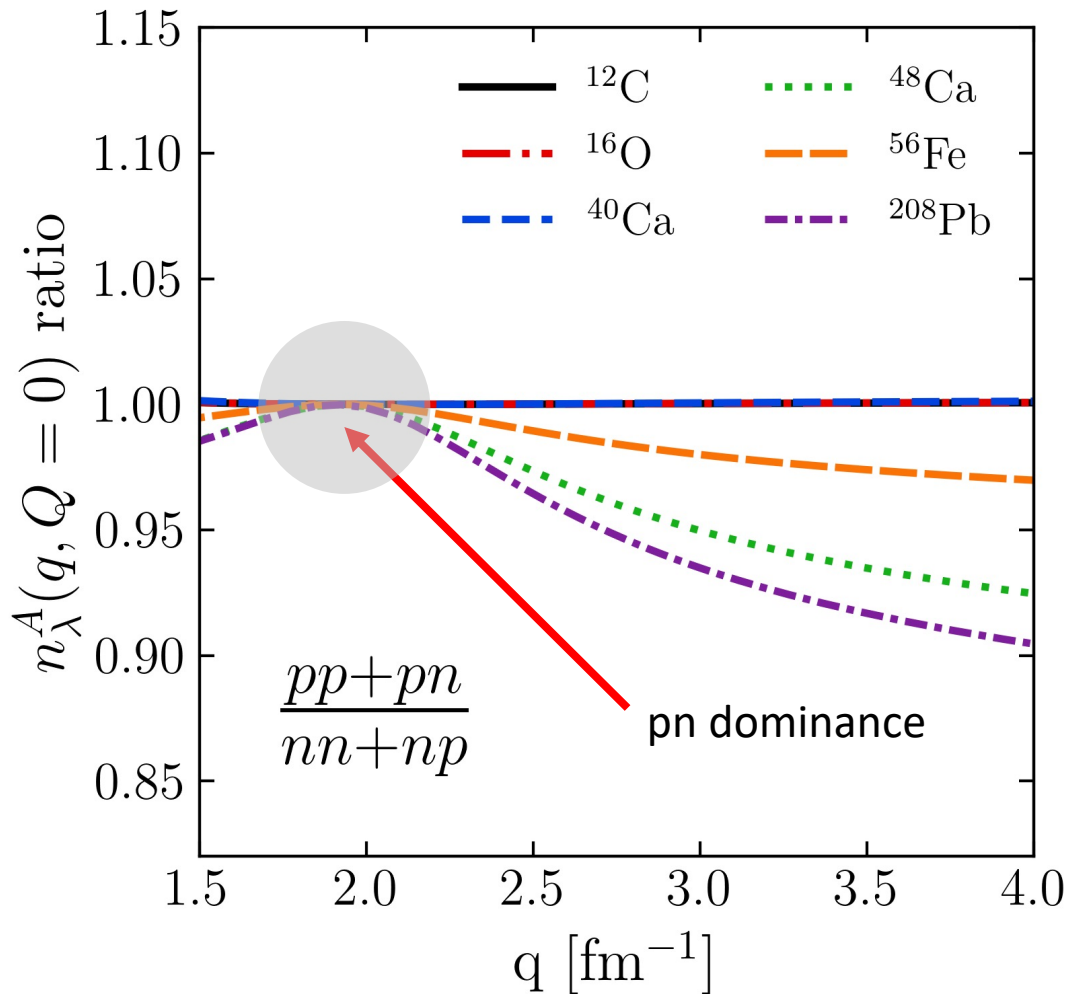
LDA results



- Reproduces the characteristics of cross section ratios using **low RG resolution operator with simple approximations**

Fig. 7: pp/pn ratio of pair momentum distributions under LDA with AV18 and $\lambda = 1.35 \text{ fm}^{-1}$.

LDA results



- Ratio ~ 1 independent of N/Z in pn dominant region
- Ratio < 1 for nuclei where $N > Z$ and outside pn dominant region

Fig. 8: $(pp+pn)/(nn+np)$ ratio of pair momentum distributions under LDA with AV18 and $\lambda = 1.35 \text{ fm}^{-1}$. Anthony Tropiano, NUCLEI 2021 Meeting

LDA results

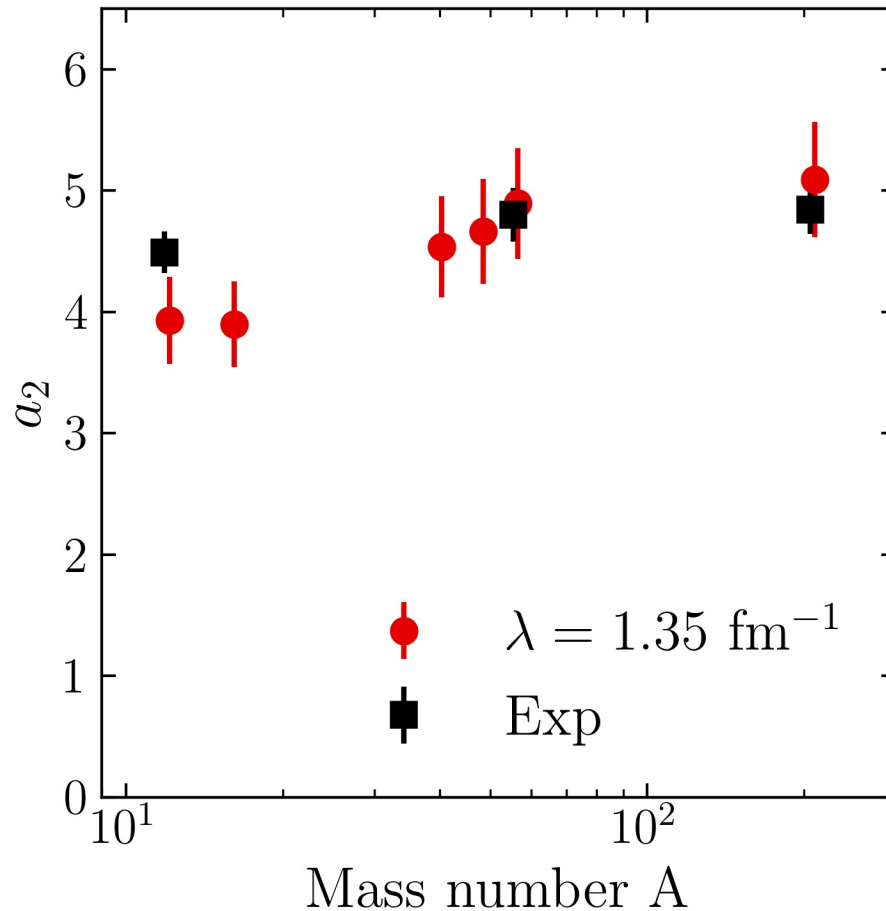


Fig. 9: a_2 scale factors using single-nucleon momentum distributions under LDA with AV18 and $\lambda = 1.35 \text{ fm}^{-1}$ compared to experimental values¹.

- SRC scale factors

$$a_2 = \lim_{q \rightarrow \infty} \frac{P^A(q)}{P^d(q)} \approx \frac{\int_{\Delta p^{high}} dq P^A(q)}{\int_{\Delta p^{high}} dq P^d(q)}$$

where $P^A(q)$ is the single-nucleon probability distribution in nucleus A with error bars from varying Δp^{high}

- Good agreement with a_2 values from experiment¹ and LCA calculations².

¹B. Schmookler et al. (CLAS), Nature **566**, 354 (2019)

²J. Ryckebusch et al., Phys. Rev. C **100**, 054620 (2019)

Summary and outlook

- Simple approximations work and are systematically improvable at low RG resolution
- Results suggest that we can analyze high-energy nuclear reactions using low RG resolution structure (e.g., shell model) and consistently evolved operators
 - Matching resolution scale between structure and reactions is crucial!
- Ongoing work:
 - Extend to cross sections and test scale/scheme dependence of extracted properties
 - Further investigate how final state interactions and physical interpretations depend on the RG scale
 - Apply to more complicated knock-out reactions (SRG with optical potentials)
 - Implement uncertainty quantification in low RG resolution calculations

Extras

Extras

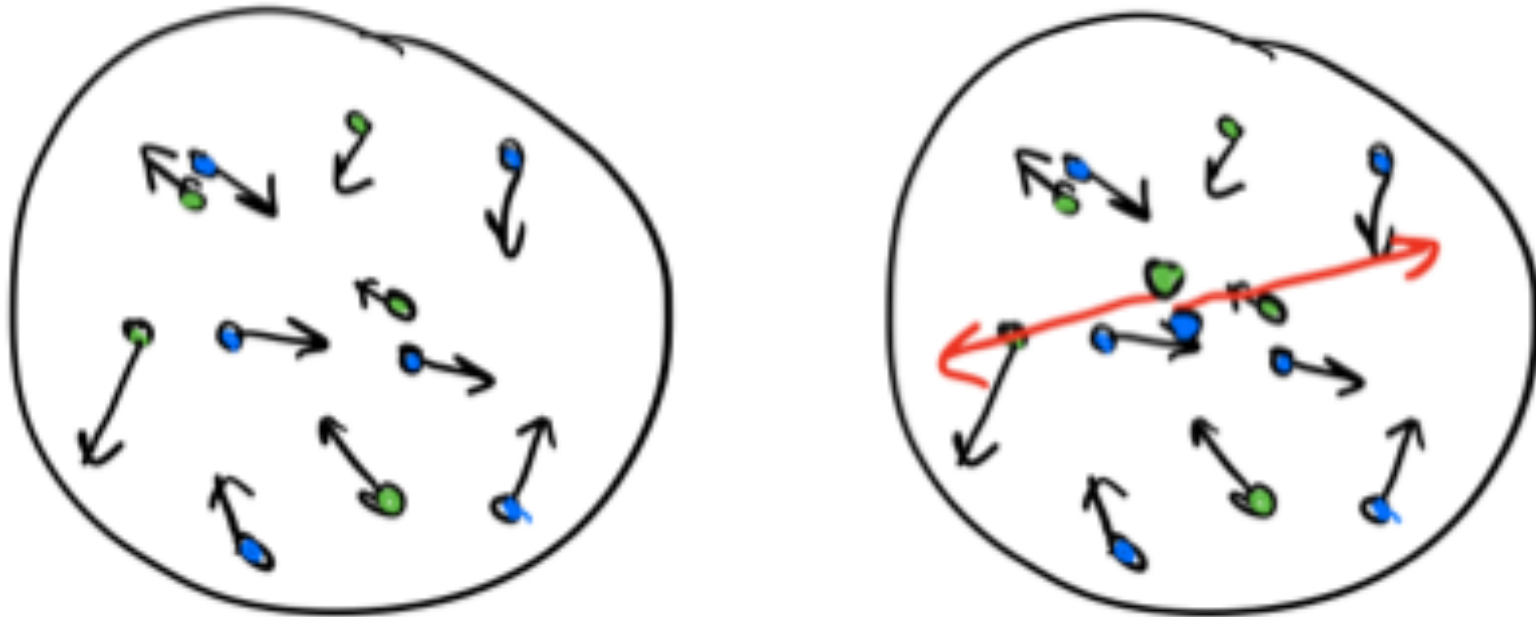


Fig. 10: Cartoon snapshots of a nucleus at (left) low-RG and (right) high-RG resolutions. The back-to-back nucleons at high-RG resolution are an SRC pair with small center-of-mass momentum.

SRG decoupling

- Evolve operators to low RG resolution

$$O(s) = U(s)O(0)U^\dagger(s)$$

where $s = 0 \rightarrow \infty$ and
 $U(s)$ is unitary

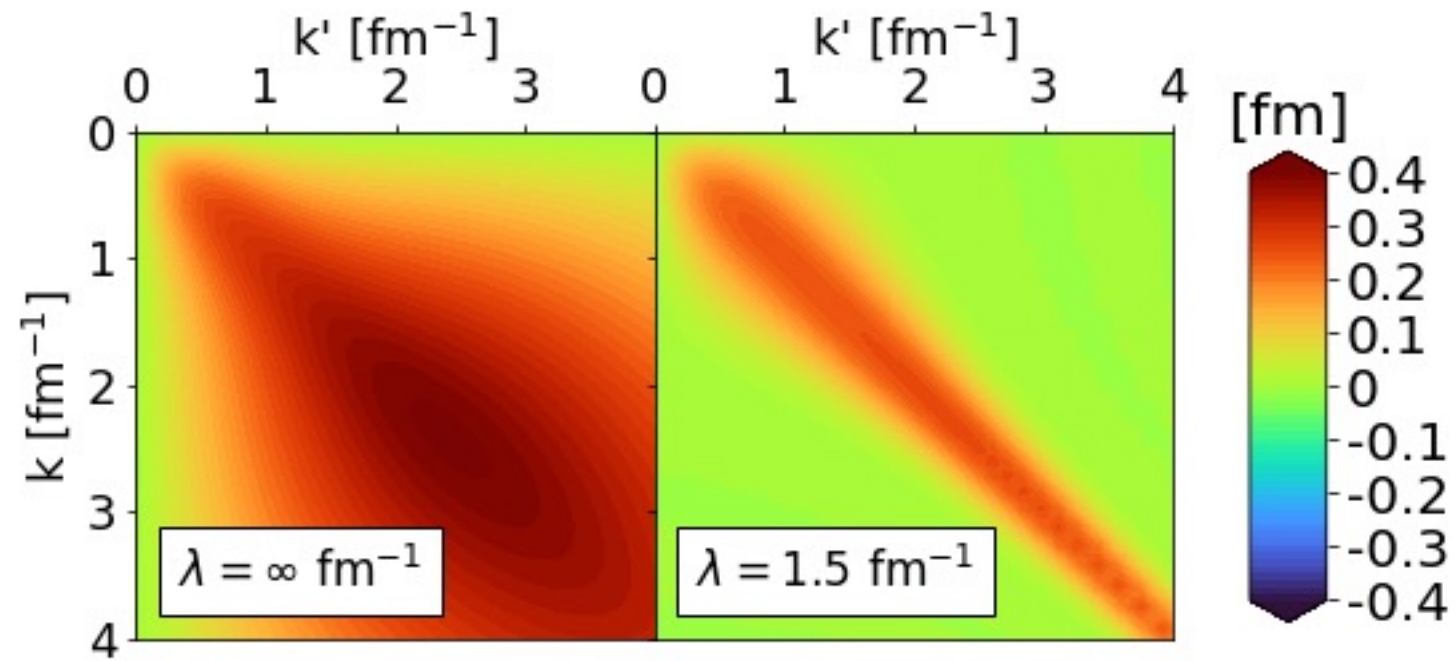


Fig. 11: Momentum space matrix elements of Argonne v18 (AV18) under SRG evolution in ${}^1\text{P}_1$ channel.

SRG decoupling

- Evolve operators to low RG resolution

$$O(s) = U(s)O(0)U^\dagger(s)$$

where $s = 0 \rightarrow \infty$ and $U(s)$ is unitary

- $\lambda = s^{-1/4}$ describes the decoupling scale of the RG evolved operator

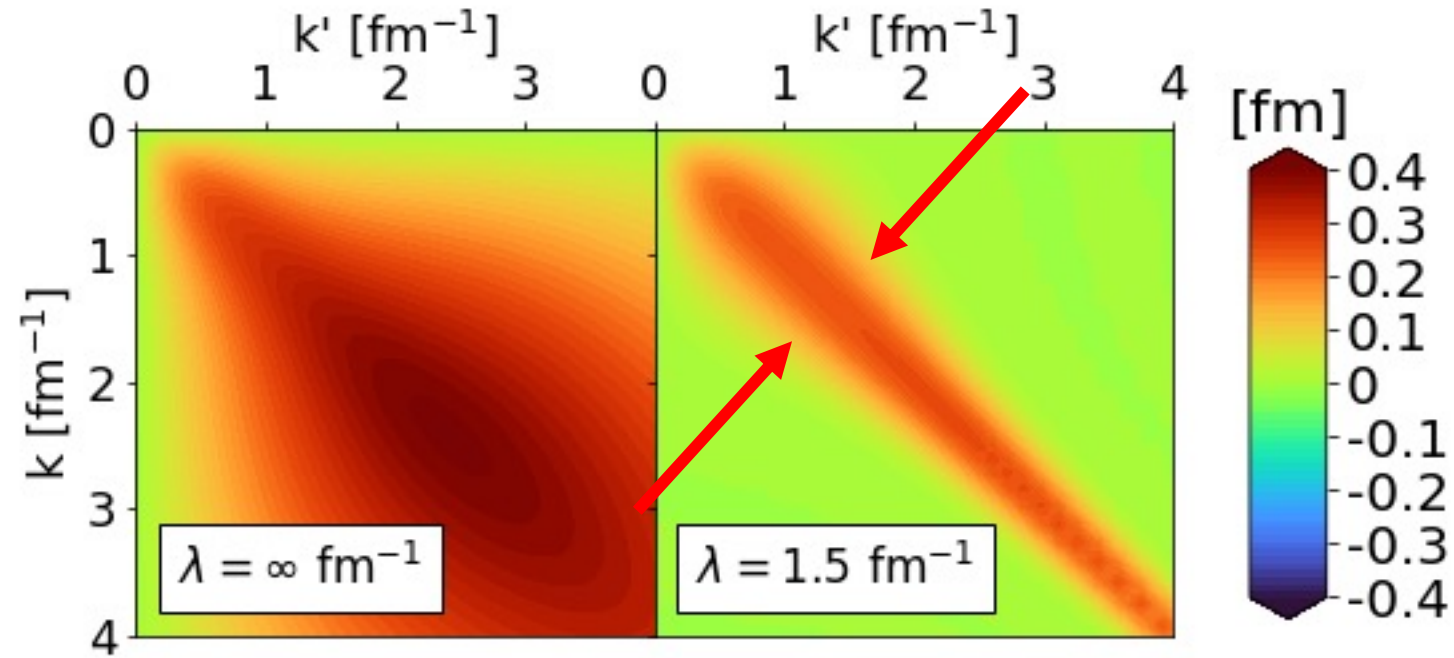
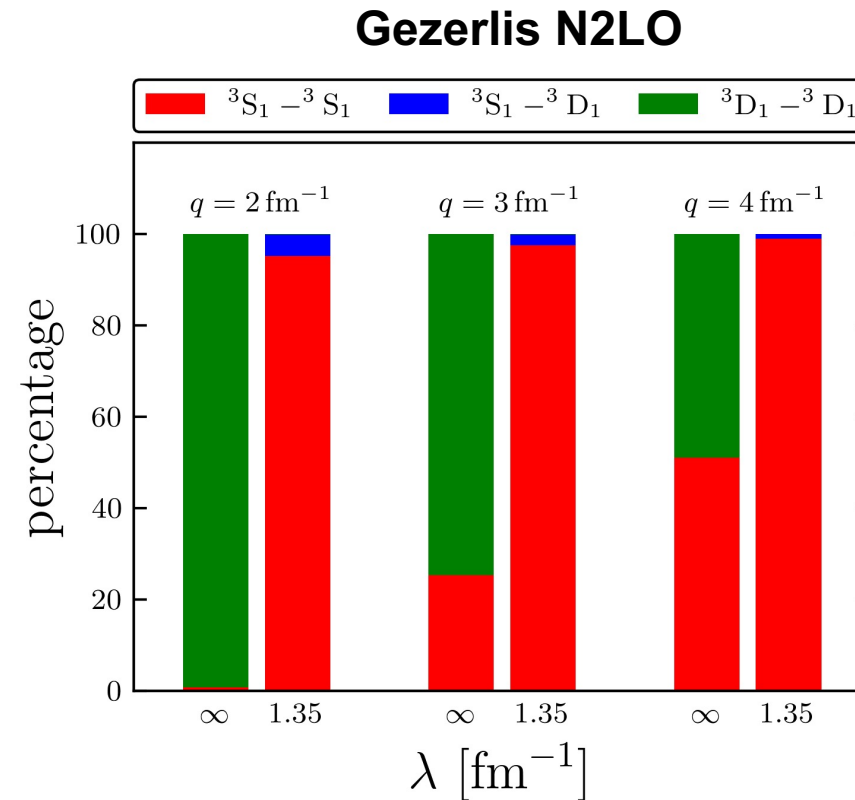
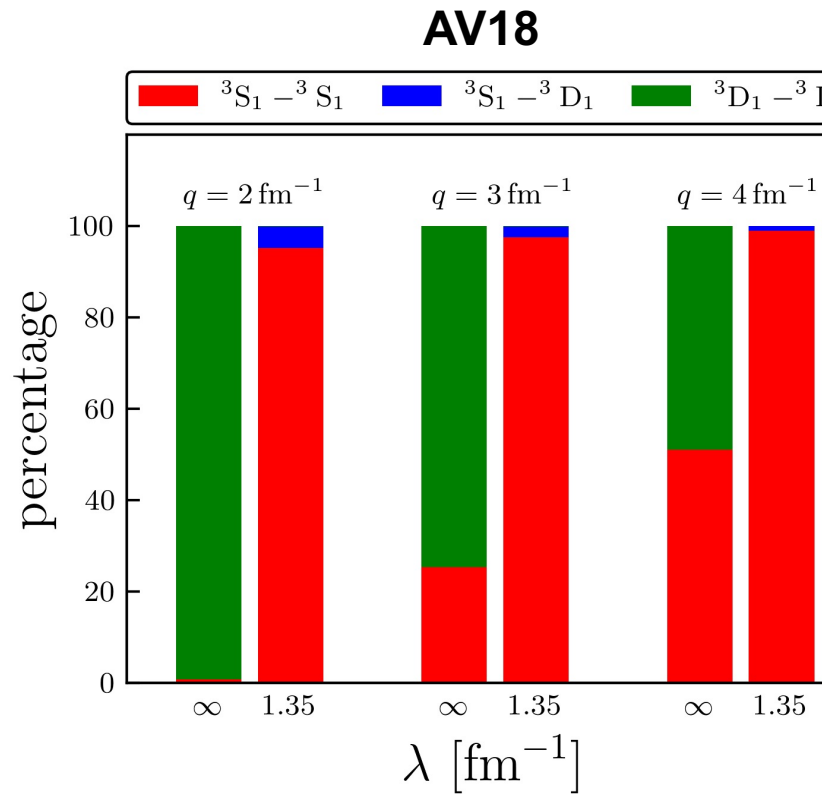
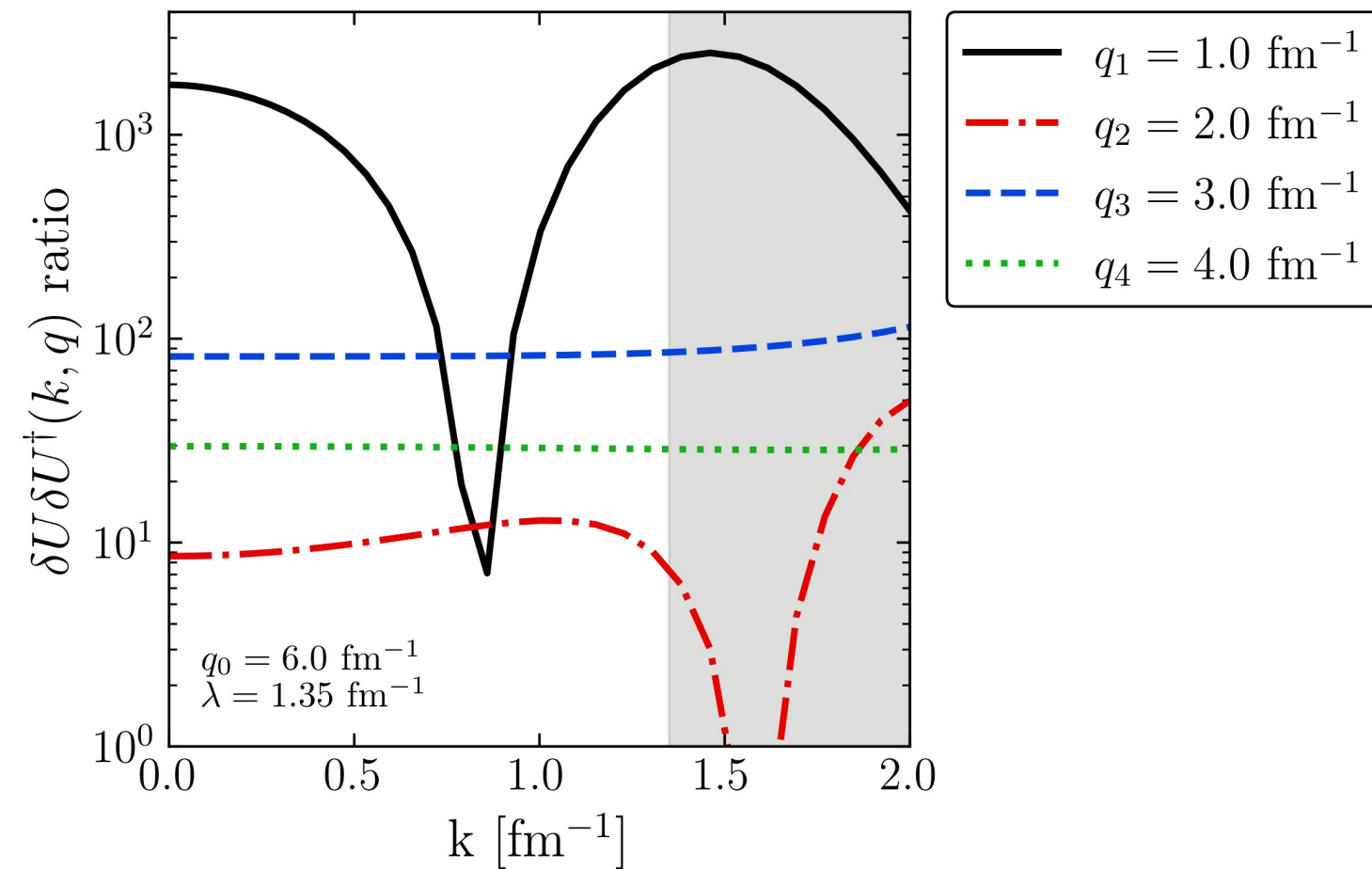
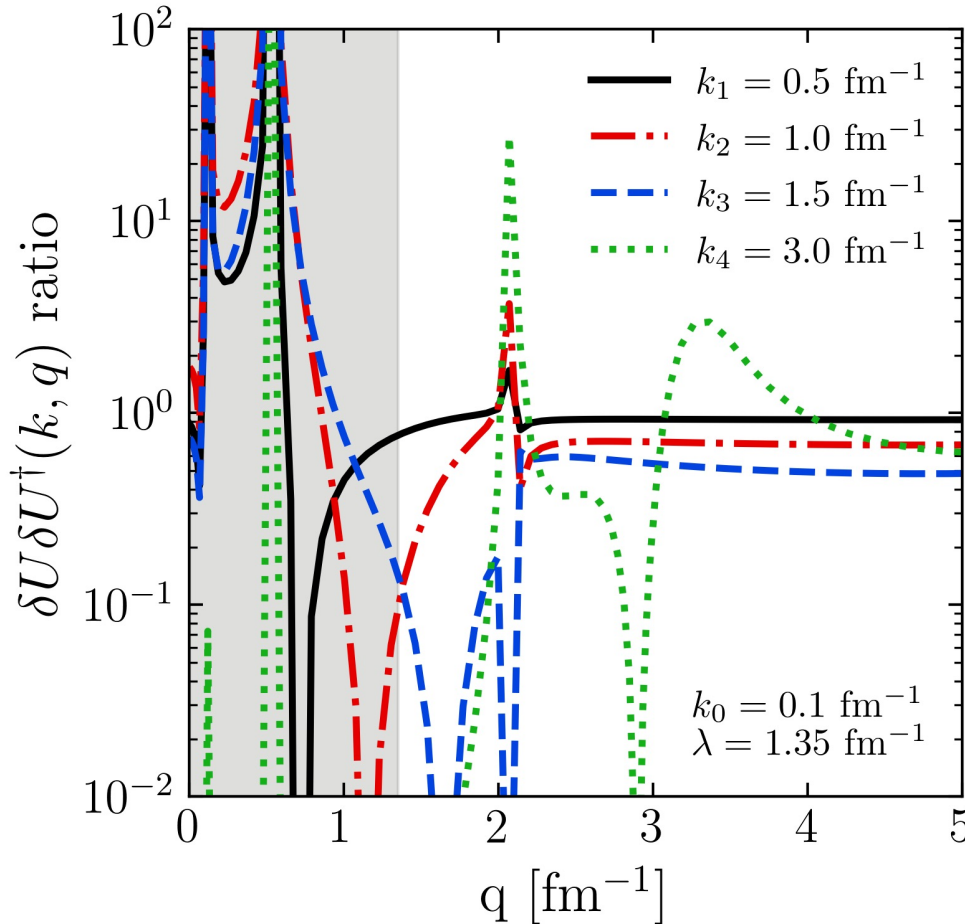


Fig. 11: Momentum space matrix elements of Argonne v18 (AV18) under SRG evolution in ${}^1\text{P}_1$ channel.

S-state and D-state contributions



Factorization



SRG λ dependence in momentum distributions

